Combustion Engines

Article · June 2021

CITATIONS
0

READS
62

9 authors, including:

Avinash Kumar Agarwal
Indian Institute of Technology Kanpur
582 PUBLICATIONS **23,244** CITATIONS
SEE PROFILE

Akhilendra Pratap Singh
Indian Institute of Technology Kanpur
102 PUBLICATIONS **3,619** CITATIONS
SEE PROFILE

Vikram Kumar
Indian Institute of Technology Kanpur
46 PUBLICATIONS **757** CITATIONS
SEE PROFILE

Nikhil Sharma
Indian Institute of Technology Kanpur
35 PUBLICATIONS **710** CITATIONS
SEE PROFILE

SAE INTERNATIONAL

ARTICLE INFO
Article ID: 03-14-06-0047

doi:10.4271/03-14-06-0047

Alcohol-Fueled Reactivity-Controlled Compression Ignition Combustion for Partial Replacement of Mineral Diesel in Internal Combustion Engines

Avinash Agarwal,[1] Akhilendra Pratap Singh,[1] Vikram Kumar,[1] Nikhil Sharma,[1] and Dev Prakash Satsangi[1]

[1]Indian Institute of Technology Kanpur, India

Abstract

In this experimental study, a novel combustion technique, "reactivity-controlled compression ignition" (RCCI), has been investigated using alcohols acting as low-reactivity fuel (LRF) and mineral diesel acting as high-reactivity fuel (HRF). Combustion experiments were performed in a single-cylinder research engine at a constant engine speed of 1500 rpm and a low engine load of 3 bar brake mean effective pressure (BMEP). RCCI combustion is a practical low-temperature combustion (LTC) concept, which was achieved using three primary alcohols: Methanol, Ethanol, and Butanol in different premixed ratios (r_p = 0.25, 0.50, and 0.75) with mineral diesel. Results showed a relatively superior performance and emissions characteristics of RCCI combustion than the conventional compression ignition (CI) combustion. The influence of LRF was visible in the RCCI combustion, which exhibited a more stable combustion than the baseline CI combustion. Retarded start of combustion (SoC) with increasing r_p was exhibited by all alcohols; however, this trend was more dominant for Methanol/diesel- and Ethanol/diesel-fueled RCCI combustion. The presence of moisture traces in Ethanol was clearly observed in Ethanol/diesel-fueled RCCI combustion. Butanol/diesel-fueled RCCI combustion showed more significant similarity with conventional CI combustion at the lower r_p. RCCI combustion-fueled with different alcohols produced relatively lower emissions of oxides of nitrogen (NOx); however, hydrocarbon (HC) and carbon monoxide (CO) emissions were higher than that of baseline CI combustion. Among different alcohols, Methanol/diesel and Ethanol/diesel showed a higher reduction in particulate matter (PM) emissions than the Butanol/diesel-fueled RCCI combustion. At higher r_p, particulate characteristics of RCCI combustion were similar to that of spark ignition (SI) engines. Correlation between the total particulate mass (TPM) and the NOx emissions showed a strong possibility of significant emission reduction by employing RCCI combustion in the engines while ensuring energy diversification and use of biofuels in an efficient manner.

History

Received: 03 Jul 2020
Revised: 07 Feb 2021
Accepted: 21 Apr 2021
e-Available: 12 May 2021

Keywords

Reactivity-controlled compression ignition, Particulate matter, Methanol, Ethanol, Butanol

Citation

Agarwal, A., Singh, A., Kumar, V., Sharma, N. et al., "Alcohol-Fueled Reactivity-Controlled Compression Ignition Combustion for Partial Replacement of Mineral Diesel in Internal Combustion Engines," *SAE Int. J. Engines* 14(6):2021, doi:10.4271/03-14-06-0047.

ISSN: 1946-3936
e-ISSN: 1946-3944

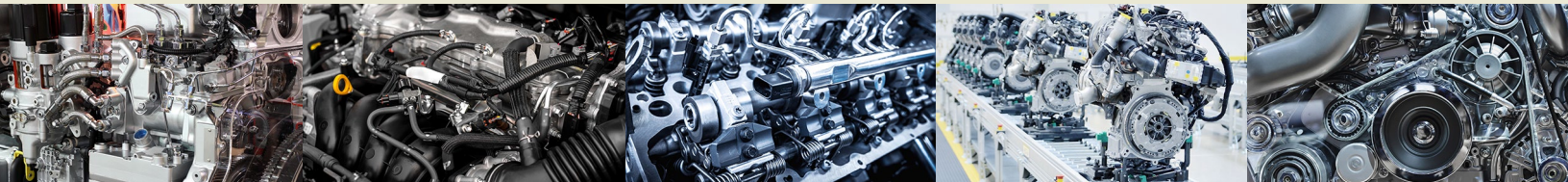

1. Introduction

Due to the rapid growth of transport energy demand and serious concerns for a clean environment, the development of efficient and cleaner engine technologies and engines has become a necessity for various sectors such as road transport, agriculture, etc. Currently, diesel-fueled compression ignition (CI) engines are the first choice in these sectors due to their higher efficiency than the spark ignition (SI) engines. However, CI engines suffer from a major drawback of higher exhaust emissions of oxides of nitrogen (NOx) and particulate matter (PM). Many studies have shown that NOx and PM emitted from CI engines are harmful to the human health as well as to the environment, and the World Health Organization (WHO) has termed diesel particulates as "Carcinogenic" [1]. NOx-PM trade-off is a major challenge for diesel engines [2]. In the last few decades, many exhaust gas aftertreatment devices such as diesel oxidation catalysts, diesel particulate filters, selective catalytic reduction, lean NOx traps, etc. have been developed to control these pollutants. However, system complexity, cost, reliability, operational constraints, etc. remain major concerns, which limit their application for many diesel engine segments. Therefore it becomes necessary to explore advanced combustion technologies for diesel engines, delivering higher thermal efficiency and lower NOx and PM emissions simultaneously [3].

Low-temperature combustion (LTC) technologies reduce NOx and PM emissions simultaneously by lowering the peak in-cylinder temperature and fuel-rich zones inside the engine combustion chamber [4]. Homogeneous-charge compression ignition (HCCI) and premixed-charge compression ignition (PCCI) combustion are the two most popular LTC modes, which have significant potential to reduce NOx and PM emissions simultaneously [5, 6, 7]. However, the lack of combustion control and very high heat release rate (HRR) at higher engine loads remain two critical issues, due to which these combustion techniques have not been implemented in commercial production engines thus far [8, 9]. In the last few years, another novel LTC concept, "reactivity-controlled compression ignition" (RCCI) combustion, has attracted significant attention from the researchers worldwide due to its superior combustion control and performance characteristics in comparison to other LTC techniques. In RCCI combustion, two fuels, one being low-reactivity fuel (LRF) and the other being high-reactivity fuel (HRF), are used to produce a reactivity gradient of the combustible charge in the engine combustion chamber [10]. LRF could be a liquid or gaseous fuel (lower cetane number [CN]), which could be injected into the intake manifold at very low fuel injection pressure (FIP) to create a lean homogeneous charge. The HRF (higher CN) is injected directly into the engine combustion chamber at high FIP. A combustible mixture of these two fuels inside the engine combustion chamber controls the HRR and combustion phasing (CP). The ratio of these two fuels (premixed ratio [r_p]) is a key parameter that controls the charge's global reactivity. In RCCI combustion, global charge reactivity plays an important role and influences combustion events such as the start of combustion (SoC) and CP [11]. Reactivity stratification is another important parameter controlled by fuel spray penetration and entrainment of HRF with the premixed charge of LRF and air. Reactivity stratification controls the combustion duration (CD), which reduces with increasing reactivity stratification [12]. Kokjohn et al. [13, 14] performed RCCI experiments using gasoline (RON = 95.6)/mineral diesel (CN = 46.1) fuel-pair. They reported limited control over the autoignition, especially at higher engine loads. It was reported that RCCI combustion using lower r_p of LRF was suitable in the low-to-medium load range. However, for higher engine loads, a r_p was required to be increased to achieve a trade-off between the combustion and emission characteristics of RCCI combustion.

Combustion, performance, and emission characteristics of RCCI combustion were investigated by many researchers using various combinations of LRF and HRF such as gasoline-diesel and gasoline-gasoline with cetane improver, and E85 (Ethanol 85%+gasoline 15%)-diesel, hydrous ethanol-diesel, etc. [15, 16, 17, 18]. Many researchers explored the use of hydrous Ethanol in advanced combustion modes. They reported that Ethanol with moisture traces exhibited a more efficient combustion along with relatively lower life-cycle carbon dioxide (CO_2) emissions. [18]. Hanson et al. [19] performed RCCI experiments using a diesel/gasoline fuel-pair. They reported that the start of injection (SoI) timing of the HRF was a critical parameter for controlling NOx and PM emissions. At retarded SoI timings, heterogeneous fuel-air mixing led to higher NOx and PM emissions than the advanced SoI timings of HRFs. At advanced SoI timings, relatively smoother combustion was observed due to the lower pressure rise rate (PRR), which was another important finding of their study. Splitter et al. [20] and Curran et al. [21] investigated the effect of fuel reactivity on the RCCI combustion. They used a mixture of Ethanol and gasoline (E85) as LRF to increase the reactivity gradient for obtaining superior RCCI combustion. Among different fuel-pairs, alcohol-diesel was the most explored fuel-pair due to its excellent RCCI combustion characteristics, higher engine efficiency, and extended engine load limits. This is the most attractive feature of RCCI combustion, in which alternative fuels can be utilized efficiently along with the significant reduction in NOx and PM emissions [16]. The use of alcohols as LRF in RCCI combustion reduces petroleum consumption by direct replacement of mineral diesel. Methanol, Ethanol, and Butanol are the three important primary alcohols, which have been explored as fuel in RCCI combustion. The presence of inherent oxygen in these alcohols promotes the oxidation of HC, CO, and PM. Dempsey et al. [15] performed RCCI experiments using a diesel/Methanol fuel-pair and reported that high octane number and high latent heat of vaporization (LHV) resulted in a retarded CP, which deteriorated the engine performance. To maintain an optimum CP, the fraction of HRF was increased significantly, which resulted in higher NOx and PM emissions. In another study carried out by Dempsey et al. [22], the effect of hydrated ethanol was explored in the RCCI mode combustion. They emphasized that the presence of moisture in ethanol improved the combustion stability and reduced the in-cylinder

temperature. They also reported that hydrated ethanol was unsuitable for conventional combustion engines; however, it can be used in RCCI mode combustion engines. Zou et al. [23] performed numerical investigations of RCCI combustion mode fueled with Methanol, Ethanol, and n-Butanol as LRF and mineral diesel as HRF. They found that NOx and soot emissions decreased with increasing LRF fraction at low-load conditions. At higher engine loads, increasing the fuel oxygen content resulted in a dominant reduction in soot emissions; however, reduction in NOx emissions was not significant. Tuner [24] also explored the use of alternative fuels in conventional and advanced engine concepts with emphasis on efficiency improvement and emission reduction. Isik and Aydin [25] compared RCCI combustion characteristics of a diesel/Ethanol fuel-pair with a biodiesel/Ethanol fuel-pair. They reported that the biodiesel/Ethanol fuel-pair was more efficient than the diesel/Ethanol fuel-pair due to the presence of fuel-bound oxygen in biodiesel/Ethanol fuel-pair, which eliminated the soot formation and resulted in lower heat losses. Hanson et al. [26] performed RCCI experiments using E20 (20% v/v Ethanol blended with gasoline)/biodiesel fuel-pair. A significant improvement in the combustion and performance characteristics of E20 as LRF was the main conclusion of this study. They reported that the engine load limit could be extended by using an E20/biodiesel fuel-pair due to a greater reactivity gradient than the gasoline/diesel fuel-pair. Fang et al. [27] used a hydrous Ethanol/diesel fuel-pair to achieve the RCCI combustion. They successfully replaced ~80% of the total fuel energy with hydrous Ethanol and improved engine performance with lower NOx and PM emissions. Increased HC and CO emissions from RCCI combustion was a common conclusion from numerous studies on RCCI combustion. However, bioethanol/biodiesel RCCI combustion resulted in slightly higher HC emissions than other test fuels [28]. Few researchers used B20 (20% v/v Butanol blended with mineral diesel) as HRF and reported that B20/gasoline-fueled RCCI combustion characteristics were similar to diesel/gasoline-fueled RCCI combustion [29, 30]. However, the use of B20 as HRF resulted in relatively lower r_p than the baseline mineral diesel. Butanol's presence was the main reason for this behavior, which reduced the reactivity gradient, leading to a narrower window of the r_p.

Particulate characteristics of three different combustion modes, namely, CI, PCCI, and RCCI, were investigated by Prikhodho et al. [31]. They reported significantly lower PM emissions from RCCI combustion than the CI combustion. However, PM emissions were relatively higher than the PCCI combustion. They suggested that the accumulation of higher volatile HCs on the filter paper was the main reason for relatively higher PM mass emissions from RCCI combustion than the PCCI combustion. Zheng et al. [30] investigated PM emission characteristics of RCCI combustion using Butanol and Ethanol as LRF. They reported that Butanol/diesel-fueled RCCI combustion emitted a relatively higher PM mass emissions than Ethanol-fueled RCCI combustion. A higher CN of Butanol was the main reason for this behavior, resulting in a shorter ignition delay than Ethanol, leading to inferior fuel-air mixing.

In previous studies, different alcohols were used as LRF to achieve RCCI combustion, and most studies focused on combustion, performance, and emission investigations of RCCI combustion. Very few studies are available in the open literature in which a comparative investigation of RCCI combustion using different alcohols has been reported. However, detailed PM characteristics of RCCI combustion using different alcohols have not been reported in any article available in the open literature. Therefore, this study focuses on RCCI combustion using different alcohols such as Methanol, Ethanol, and Butanol as LRF and mineral diesel as HRF. RCCI combustion experiments were performed in a single-cylinder research engine at a constant engine speed (1500 rpm) and low engine load (3 bar brake mean effective pressure [BMEP]). RCCI combustion experiments were performed at three different premixed ratios (r_p = 0.25, 0.50, and 0.75), and r_p = 0 represents CI combustion. For all experiments, fuel injection parameters such as FIP and start of main injection timings of the HRF were kept constant at 500 bar and 17° crank angle before top dead center (CA bTDC), respectively. Detailed PM characterization is an important aspect of this study, which included particle number-size distribution, particle mass-size distribution and number concentrations of total particles, nucleation mode particles (NMP, D_p < 50 nm), and accumulation mode particles (AMP, 50 nm < D_p < 1000 nm). Qualitative correlations between particle number and mass, total particulate mass (TPM), and NOx emissions are a few novel aspects investigated in this experimental study, demonstrating RCCI combustion's effectiveness over conventional CI combustion. Relatively better suitability of Methanol and Ethanol as LRF in RCCI combustion mode than Butanol is another important finding of this study.

2. Experimental Setup

A single-cylinder, four-stroke, direct injection compression ignition engine (AVL; 5402) was used for experimental investigations of RCCI combustion in this study. This engine was a single-cylinder version of a multi-cylinder engine equipped with a high-pressure common-rail direct injection (CRDI) system and could inject fuel up to 1400 bar in as many as four injections in an engine cycle. A schematic of the experimental setup is shown in Figure 1.

Technical specifications of the test engine are given in Table 1.

For the engine experiments, an AC dynamometer (Wittur Electric Drives GmbH, Germany; 2SB 3) was used to control the engine speed and load. A dedicated engine management system was used for controlling the injection (DI) parameters such as FIP, quantity, timing, number of injections, etc. This system included an electronic control unit (ECU), a communication interface (ETAS, ETK 7.1 Emulator probe), and a control program (INCA). Using this system, up to four injections per engine cycle could be done. The experimental setup

FIGURE 1 Schematic of the experimental setup.

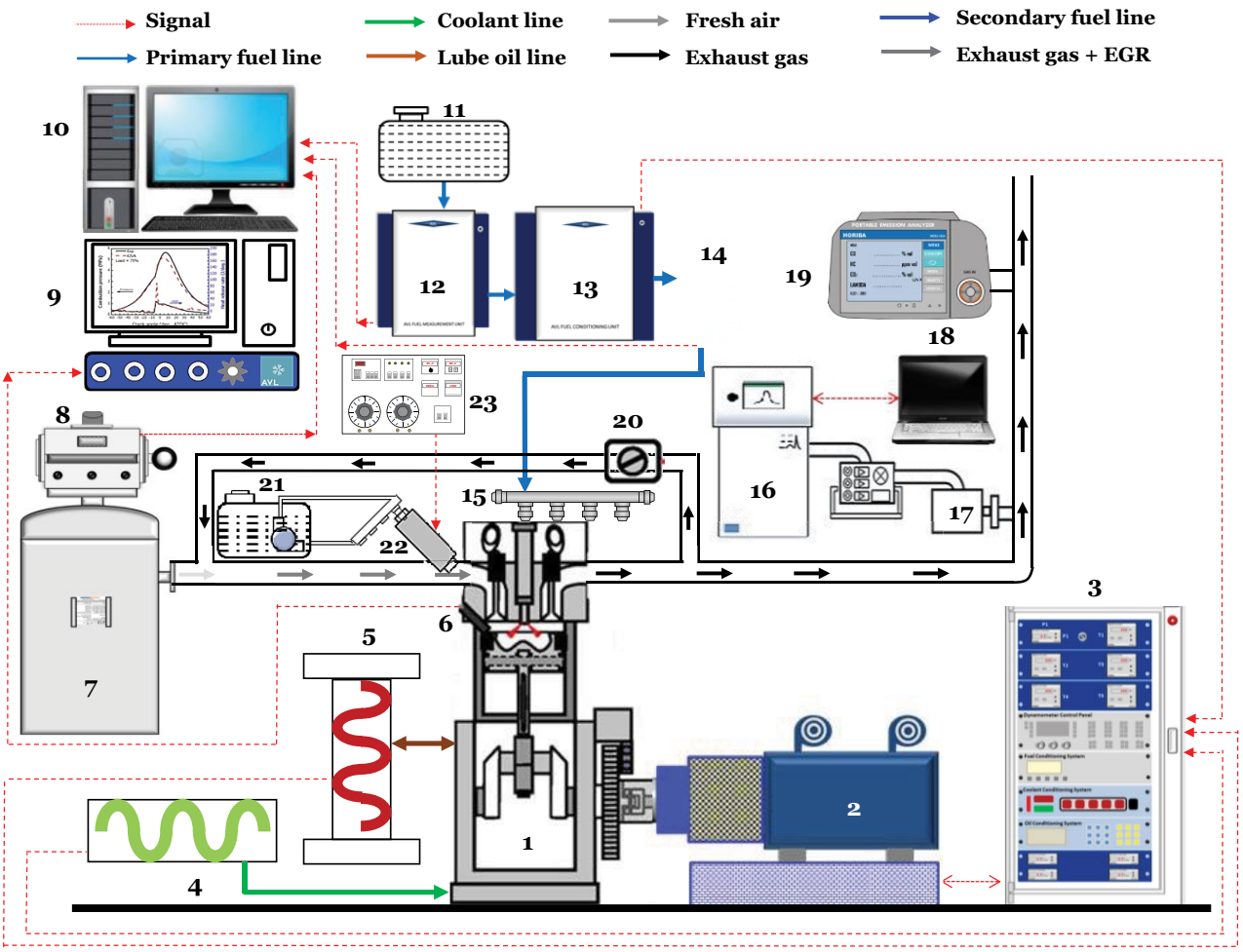

1	Test engine	2	Transient dynamometer	3	Control panel
4	Coolant conditioning system	5	Lubricating oil conditioning system	6	Pressure transducer
7	Intake air surge tank	8	Air-flow measurement system	9	Data acquisition system
10	ECU interface system	11	Primary fuel tank	12	Fuel measurement system
13	Fuel conditioning system	14	High-pressure fuel pump	15	High-pressure common rail
16	Engine exhaust particle sizer	17	Thermo diluter and air pump	18	EEPS data logger
19	Raw exhaust gas analyzer	20	EGR regulator	21	Secondary fuel tank
22	Port fuel injector	23	Injection driver		

consisted of another fuel injection system for port fuel injection, which was operated at a relatively lower FIP (3 bar). This system consisted of an electric fuel pump, a fuel tank, a fuel accumulator, a fuel injector (Denso; 1500M844M1), and a fuel injector control circuit. Details of the fuel injection driver circuit could be seen in our previous publication [32].

For performing the experiments under controlled conditions, the test engine was equipped with three conditioning systems, namely, fuel condition system (AVL, 553), lubricating oil conditioning system (Yantrashilpa; YS4312), and coolant conditioning system (Yantrashilpa; YS4027). These systems maintain pressure and temperatures of the test fuel, lubricating oil, and coolant, respectively, so that uncertainties can be avoided during the experiments. During the RCCI experiment, lubricating oil, fuel, and coolant temperatures were maintained constant at 90°C, 25°C, and 60°C, respectively. For measuring the injected fuel quantity of the HRF, a gravimetric fuel metering unit (AVL, 733S) was used. For controlling the HRR of RCCI combustion, an exhaust gas recirculation (EGR) system was used. In this system, a fraction of exhaust gas was recirculated back into the intake system, mixed with fresh intake air, before being supplied to the engine combustion chamber. In this study, an EGR regulator was used to supply a fixed EGR quantity (15% EGR) for both

TABLE 1 Specifications of the test engine.

Engine make/model	AVL/5402
Number of cylinder/s	1
Cylinder bore/stroke	85/90 mm
Swept volume	510.7 cc
Compression ratio	17.0
Inlet ports	Two (one tangential port and one swirl port)
Nominal swirl ratio	1.78
Maximum power output	6 kW
Rated speed	4200 rpm
Fuel injection pressure	200-1400 bar
Fuel injection system	Common rail direct injection
Split fuel injection capability	Two pre-injections, one main injection, and one post-injection
High-pressure system	BOSCH Common Rail CP4.1
Engine management system	AVL-RPEMS + BOSCH ETK7
Valves per cylinder	4 (2 inlet, and 2 exhaust)

RCCI combustion mode and baseline CI combustion mode. EGR temperature was measured before mixing with fresh intake air. The intake air temperature was maintained constant at 40±2°C. For measuring the intake air flow rate, an air measurement system (ABB Automation Products, Sensyflow P) was installed in the experimental setup. For measuring the EGR flow rate, an orifice plate and a U-tube manometer were installed in the EGR line.

For in-cylinder combustion analysis, a water-cooled piezoelectric pressure transducer (AVL, QC34C) was mounted flush in the engine cylinder head. This pressure transducer measured the in-cylinder pressure up to 250 bar. For crank position measurement, a precision optical shaft encoder (AVL, 365C) was installed onto the engine crankshaft. Signals of the pressure transducer and angle encoder were acquired by a high-speed combustion data acquisition (DAQ) system (AVL, IndiMicro). This DAQ system processed raw signals and provided the in-cylinder pressure and other derived combustion parameters with respect to (w.r.t.) the CA position. Other important details of in-cylinder pressure analysis could be seen in our previous publication [33]. For exhaust gas characterization, two emission measurement equipment, namely, (i) raw exhaust gas emission analyzer (Horiba; 584L) and (ii) engine exhaust particle sizer (EEPS) spectrometer (TSI; 3090), were used. Raw exhaust gas emission analyzer measured concentrations of regulated gaseous species such as CO, HC, CO_2, and NOx. EEPS measured the number-size distribution of particles present in the exhaust gas. It can measure up to #10^8 particles/cc of exhaust in 5.6-560 nanometer size range. Other important details of the EEPS can be seen in our previous publication [34].

Important fuel properties such as density, kinematic viscosity, and calorific value of HRF (mineral diesel) and LRFs (Methanol, Ethanol, and Butanol) were measured using a portable density meter (Kyoto Electronics; DA130N), viscometer (Stanhope-Seta; 83541-3), and bomb calorimeter (Parr; 6200), respectively (Table 2). A few fuel properties, such as LHV, CN, etc., were taken from the literature [35, 36, 37]. Commercial-grade Ethanol was used in the experiments, which contained relatively higher moisture traces (~1-2%) than other alcohols [38].

For comparing the combustion, performance, and emission characteristics of RCCI combustion fueled with primary alcohols, experiments were performed at constant engine speed (1500 rpm) and load (3 bar BMEP). This engine load was selected based on the engine combustion and performance characteristics, which were optimum at a low engine load (3 bar BMEP). At a lower engine load, RCCI combustion showed significantly higher HC and CO emissions due to misfiring; however, at a higher engine load, CI combustion resulted in higher knocking. For RCCI experiments, the r_p, which was defined as the ratio of the port-injected fuel energy to the total fuel energy, was varied (r_p = 0.25, 0.50, and 0.75), whereas for the baseline CI combustion r_p = 0. The LRF was not injected into the port. The following formula was used to calculate r_p:

$$r_p = \frac{m \times (LHV)_{LRF}}{M \times (LHV)_{HRF} + m \times (LHV)_{LRF}}$$

where M and m are the mass flow rates of HRF and LRF. LHV is the lower heating value of the test fuels. The premixed ratios of the alcohols were decided based on energy replacement. Due to different calorific values of test fuels, the injected fuel

TABLE 2 Test fuel composition and important fuel properties.

Test fuel	Mineral diesel	Methanol	Ethanol	Butanol
Lower calorific value (MJ/kg)	44.26	21.90	28.16	31.46
Kinematic viscosity (mm^2/s) at 40°C	2.96	0.57	1.05	2.52
Density (g/cm^3) at 30°C	0.837	0.787	0.794	0.831
Latent heat of vaporization (kJ/kg)	233	1100	920	716
Cetane number	48	5	5-8	25
Octane number	—	109	107	96
C:H:O (%)	—	37.5:12.5:50	52.2:13:34.8	64.9:13.5:21.6

quantity of all test fuels was different. In all experiments, mineral diesel was injected at 500 bar FIP, and the SoI timing was kept constant at 17° CA bTDC. During the experiments, a 15% EGR rate was used to control the combustion and HRR.

3. Results and Discussion

The experimental results are divided into four sub-sections: combustion, performance, emissions, and particulate characteristics. In each sub-section, results are discussed considering two aspects: first, a comparison between RCCI combustion and baseline CI modes, and, second, a comparison of RCCI combustion using different primary alcohols as LRF.

3.1. Combustion Characteristics

In-cylinder combustion analysis is an important parameter to analyze the effectiveness of any novel combustion technique. Here the combustion analysis was done by measuring the in-cylinder pressure w.r.t. the CA position. Using this in-cylinder pressure data, other combustion parameters such as HRR, SoC, CP, CD, etc., were calculated using the First Law of Thermodynamics [39]. In this study, in-cylinder pressure data was acquired by averaging the instantaneous pressure signals of 250 consecutive cycles with a resolution of 0.1 crank angle degrees (CAD). Therefore the average data set of these 250 data sets was used for further analysis in order to minimize the effect of cyclic variations. Figure 2 shows the variations of in-cylinder pressure (thin lines) and HRR (thick lines) w.r.t. CAD at different r_p of Methanol, Ethanol, and Butanol at constant engine speed (1500 rpm), and load (3 bar BMEP).

The difference between CI and RCCI combustion characteristics is clearly visible in Figure 2. The separation of the in-cylinder pressure curve with the motoring pressure curve shows the SoC. At all r_p, the retarded SoC of RCCI combustion than the CI combustion is a common attribute for all alcohols. Among different fuel-pairs, Methanol/diesel- and Ethanol/diesel-fueled RCCI combustion showed similar combustion characteristics; however, Butanol/diesel-fueled RCCI combustion was closer to the baseline CI combustion. A relatively higher calorific value and a higher CN of Butanol than other alcohols (Methanol and Ethanol) may be a possible reason, leading to relatively lower reactivity gradient between Butanol and mineral diesel. At a lower premixed ratio ($r_p = 0.25$), peak in-cylinder pressure of alcohol/mineral diesel-fueled RCCI combustion was slightly higher than the baseline CI combustion. This was mainly due to the contributions of LRF, which hampered the combustion kinetics of the fuel-air mixture and resulted in a higher ignition delay.

HRR also showed a similar trend, and the HRR of RCCI combustion was found to be slightly higher than the baseline CI combustion. Results showed that the peak HRR of Methanol/diesel was slightly higher than the peak HRR of Ethanol/diesel-fueled RCCI combustion. At a lower premixed ratio ($r_p = 0.25$), combustion knocking can be seen in the in-cylinder pressure curves of alcohol-fueled RCCI combustion; however, the knocking tendency was relatively lower than the baseline CI combustion. At higher r_p, combustion knocking decreased due to the dominant effect of LRF in the RCCI combustion. At $r_p = 0.50$, Methanol/diesel- and Ethanol/diesel-fueled RCCI combustion showed a significantly retarded SoC than the baseline CI combustion; however, Butanol/diesel-fueled RCCI combustion showed different combustion characteristics. The SoC of Butanol/diesel-fueled RCCI combustion was slightly advanced than other test fuel pairs, and peak in-cylinder pressure was relatively higher than the baseline CI combustion. Differences in the fuel properties of Butanol than Methanol and Ethanol played an important role in these combustion characteristics (Table 2). Butanol's fuel properties were similar to mineral diesel, resulting in lower reactivity stratification, leading to a slightly higher CD. The effect of fuel properties was also reflected in the global reactivity, which resulted in a relatively advanced SoC than other fuel-pairs. These combustion characteristics might be different under constant CP conditions; however, this study was not focused on constant CP. At $r_p = 0.50$, HRR trends of RCCI combustion fueled by Methanol and Ethanol did not significantly differ; however, Butanol/diesel-fueled RCCI combustion showed mixed combustion characteristics of CI and RCCI combustion modes. With increasing r_p, the SoC of Butanol/diesel-fueled RCCI combustion retarded, similar to RCCI combustion of Methanol and Ethanol (effect of LRF); however, combustion occurred much like conventional CI combustion (effect of high CN of Butanol). Dominant RCCI combustion characteristics were observed at higher r_p, where the reactivity stratification was higher, and the presence of a larger quantity of LRF showed a dominant effect on the global reactivity. At $r_p = 0.75$, Methanol and Ethanol showed a retarded SoC, and the entire combustion occurred in the expansion stroke, resulting in a more useful work output. This was mainly due to the dominant characteristics of the LRF than the HRF. This resulted in a significant reduction in global reactivity, which increased the ignition delay, leading to a retarded SoC. Relatively higher heat of vaporization of Methanol and Ethanol was another reason for in-cylinder cooling, resulting in somewhat slower chemical kinetics of fuel-air mixture. The combined effect of fuel properties and in-cylinder processes led to retarded SoC for Methanol/diesel- and Ethanol/diesel-fueled RCCI combustion. However, Butanol/diesel-fueled RCCI combustion showed slightly advanced SoC than the other test fuels. Peak in-cylinder pressure of Methanol/diesel- and Ethanol/diesel-fueled RCCI combustion was significantly lower than the baseline CI combustion. The width of HRR trends showed the CD, which was another important parameter for RCCI combustion. HRR trends showed that CD increased with increasing r_p of LRF. This was obvious because the presence of a greater quantity of LRF retarded the fuel-air chemical kinetics (due to reduction in global reactivity) and resulted in a relatively slower combustion [14]. At lower r_p, this effect was dominant in Methanol/diesel- and Ethanol/diesel-fueled RCCI combustion, and at higher r_p, all alcohols followed a similar pattern.

FIGURE 2 In-cylinder pressure and HRR variations w.r.t. CAD at different r_p of Methanol, Ethanol, and Butanol at constant engine speed (1500 rpm), and load (3 bar BMEP).

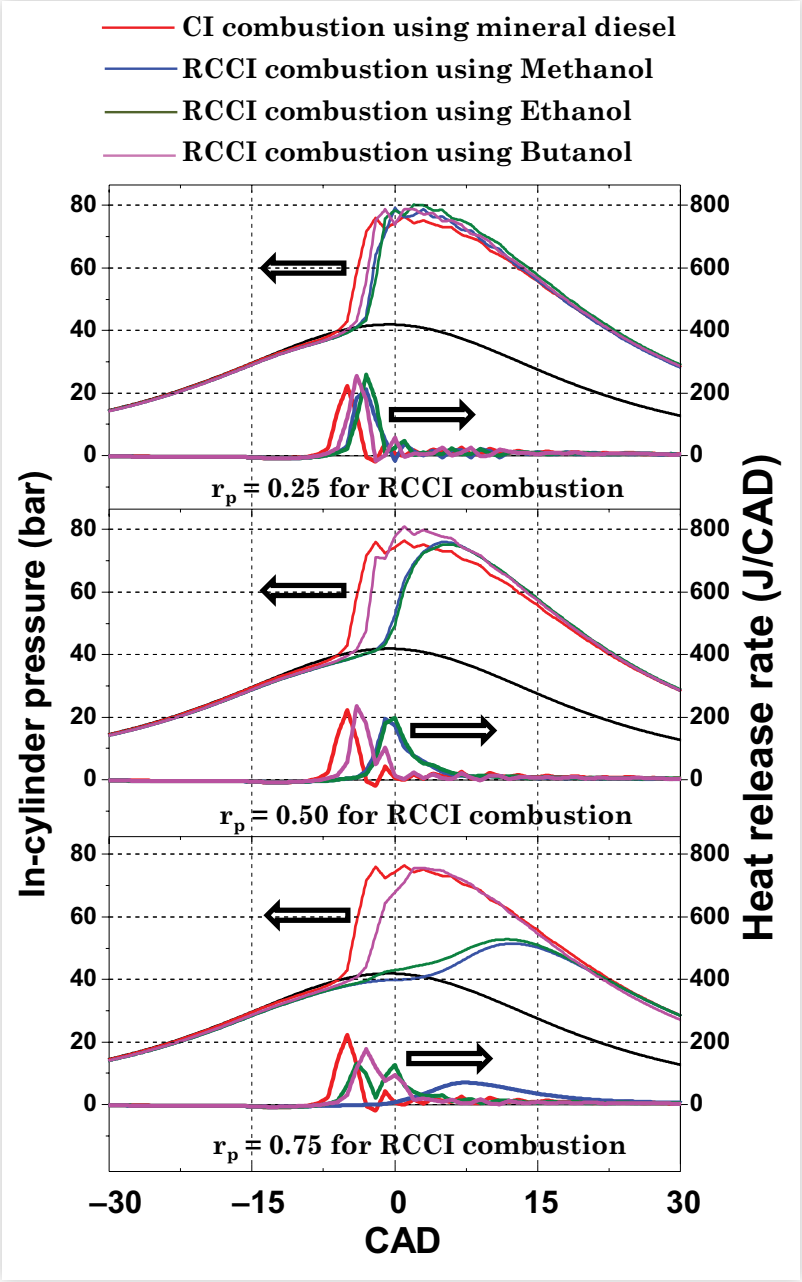

With an increasing r_p of the LRF, RCCI combustion characteristics dominated in Methanol/diesel- and Ethanol/diesel-fueled RCCI combustion; however, Butanol/diesel-fueled RCCI combustion showed proximity to the baseline CI combustion due to higher CN and higher calorific value than Methanol and Ethanol.

Figure 3 shows the variations in the SoC and CD of the baseline CI combustion and RCCI combustion at different engine loads and r_p. These parameters were calculated by mass fraction burned analysis using the Rassweiler and Withrow method [40].

$$\left(\Delta p_c\right) = p_i - p_{i-1}\left(\frac{V_{i-1}}{V_i}\right)^{\gamma}$$

where Δp_c represents the change in the in-cylinder pressure and γ is the polytropic exponent.

$$\frac{m_{b(i)}}{m_{b(total)}} = \frac{\sum_{j=0}^{i}\Delta\left(p_c\right)_j}{\sum_{j=0}^{N}\Delta\left(p_c\right)_j}$$

FIGURE 3 SoC and CD of the baseline CI combustion (red background) and RCCI combustion (green background) at different r_p of Methanol, Ethanol, and Butanol at constant engine speed (1500 rpm), and low load (3 bar BMEP).

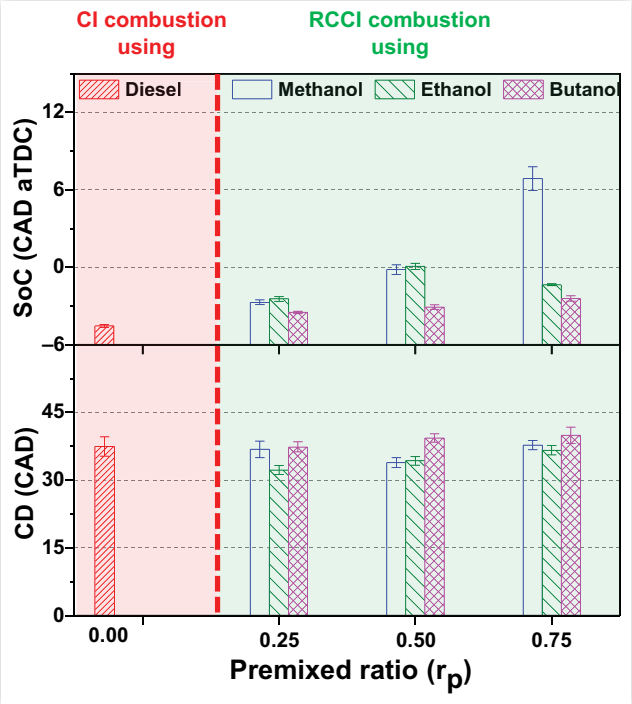

FIGURE 4 PRR, combustion noise, and KI of the baseline CI combustion (red background) and RCCI combustion (green background) at different r_p of Methanol, Ethanol, and Butanol with mineral diesel at constant engine speed (1500 rpm) and low load (3 bar BMEP).

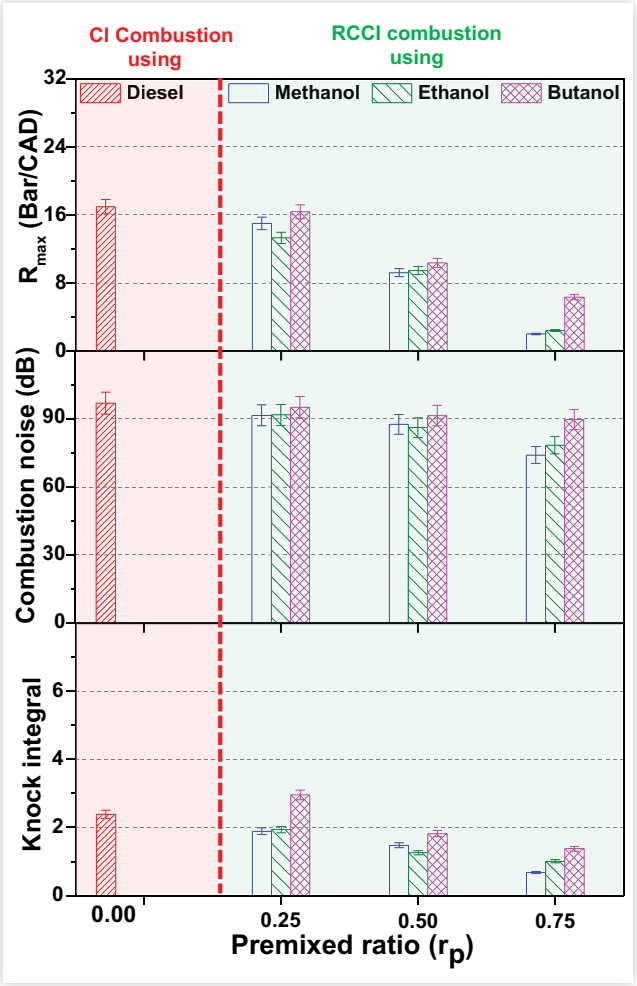

It is assumed that sample 0 is between the intake valve closing and the SoC, and sample N represents the combustion completion.

The SoC is quantified as the CA position corresponding to 10% cumulative heat release (CHR). In RCCI combustion, the SoC is affected by many parameters such as properties of LRF and HRF, engine operating conditions (speed and load), the r_p of LRF and HRF, in-cylinder conditions (temperature and pressure), intake air temperature, etc. Figure 3 shows a significantly retarded SoC of RCCI combustion than the baseline CI combustion. The effect of fuel properties on global reactivity was also visible in the RCCI combustion. Among different fuel-pairs, Methanol/diesel- and Ethanol/diesel-fueled RCCI combustion showed a more retarded SoC than the Butanol/diesel-fueled RCCI combustion. With an increasing r_p of LRF, a more retarded SoC was observed mainly due to the dominant effect of LRF, which resulted in slower fuel-air chemical kinetics (lower global reactivity) [14]. However, the effect of increasing the r_p was not significant in case of Butanol/diesel-fueled RCCI combustion. At $r_p = 0.75$, Methanol/diesel-fueled RCCI combustion resulted in the most retarded SoC. CD is the CAD difference between the end of combustion (EoC, CA position corresponding to 90% of CHR) and the SoC. The CD of RCCI combustion shows a mixed trend w.r.t. the baseline CI combustion. The CD of RCCI combustion was relatively shorter at lower r_p than the baseline CI combustion, which increased at higher r_p. It was mainly due to the dominant contribution of the LRF in fuel-air chemical kinetics, which slowed down drastically at higher r_p. Similar to the SoC and CP, the CD of Butanol/diesel-fueled RCCI combustion was different from the CD of other alcohol/diesel-fueled RCCI combustion. The CD of Butanol/diesel-fueled RCCI combustion was slightly longer than other test fuels and showed similarity with the baseline CI combustion.

Figure 4 shows the variations in the maximum rate of pressure rise (R_{max}), combustion noise, and knock integral (KI) of the baseline CI combustion, and RCCI combustion at different r_p of Methanol, Ethanol, and Butanol with mineral diesel. R_{max} is an important parameter that directly affects combustion noise and KI [38]. A lower R_{max} is desirable for LTC strategies, since it represents stable combustion. Figure 4 shows that the R_{max} of RCCI combustion was relatively lower than the baseline CI combustion, which further reduced with the increasing r_p of the LRF. The R_{max} of the baseline CI combustion was ~18 bar/CAD; however, the R_{max} of RCCI combustion at $r_p = 0.75$ was ~5 bar/CAD. Among different

fuel-pairs, Methanol/diesel- and Ethanol/diesel-fueled RCCI combustion showed a relatively lower R_{max} than the Butanol/diesel-fueled RCCI combustion. This was due to the higher reactivity gradient of Methanol and Ethanol with mineral diesel, which resulted in superior control over the combustion events. This was also in agreement with combustion noise trends.

The combustion noise of CI combustion (~100 dB) was significantly higher than the RCCI combustion (~75 dB to 90 dB). With an increasing r_p of the LRF, the combustion noise reduced. This reduction was significant at $r_p = 0.75$, at which Methanol/diesel- and Ethanol/diesel-fueled RCCI combustion resulted in a significantly lower combustion noise (~75 dB). Among different fuel-pairs, Methanol/diesel- and Ethanol/diesel-fueled RCCI combustion produced lesser combustion noise than the Butanol/diesel-fueled RCCI combustion. At a lower premixed ratio ($r_p = 0.25$), the combustion noise of Butanol/diesel-fueled RCCI combustion was similar to the combustion noise of the baseline CI combustion. KI is another parameter, which is used to characterize the combustion stability. The KI gives quantitative information about the combustion intensity, calculated by integrating the superimposed rectified knock oscillations above the threshold limit (25 bar/CAD). Results showed that the KI of RCCI combustion was lower than that of baseline CI combustion. With an increasing r_p of the LRF, KI showed a continuous reduction for all test fuels. Among different test fuel-pairs, Butanol/diesel-fueled RCCI combustion showed a slightly higher KI than other alcohols. At a lower premixed ratio ($r_p = 0.25$), Butanol/diesel-fueled RCCI combustion showed a slightly higher KI than the baseline CI combustion.

3.2. Performance Characterization

In this study, RCCI combustion experiments were performed at constant engine load (3 bar BMEP) to compare the performance characteristics, namely, brake thermal efficiency (BTE) and EGT of RCCI combustion using Methanol/diesel, Ethanol/diesel, and Butanol/diesel fuel-pairs at different r_p with the baseline CI combustion.

Figure 5 shows that the BTE of RCCI combustion using different fuel-pairs was relatively higher than the baseline CI combustion. The contribution of fuel-bound oxygen was another factor responsible for higher BTE in RCCI

FIGURE 5 BTE and EGT of the baseline CI combustion (red background) and RCCI combustion (green background) at different r_p of Methanol, Ethanol, and Butanol with mineral diesel at constant engine speed (1500 rpm), and low load (3 bar BMEP).

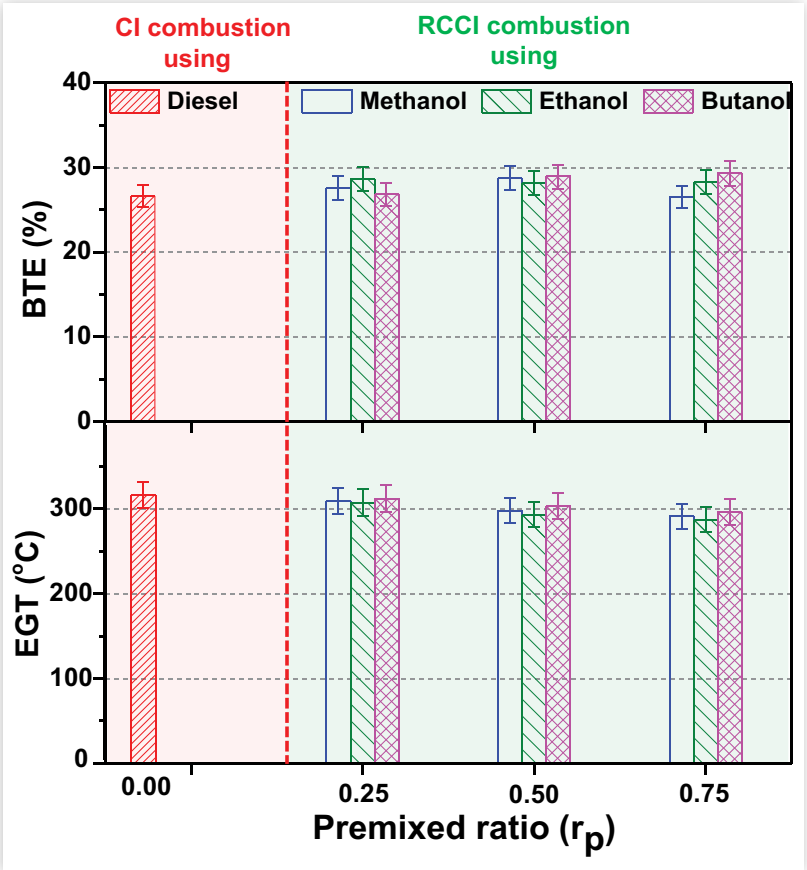

combustion mode because it promoted combustion of the test fuels. With an increasing r_p of the LRF, the BTE of RCCI combustion fueled with Methanol/diesel and Ethanol/diesel fuel pairs first increased (up to $r_p = 0.50$) and then slightly decreased. With an increasing r_p of the LRF, the dominant contribution of LRF reduced the global reactivity. This led to a retarded CP, resulting in availability of more usable power on the piston (Figure 2). The relatively lower in-cylinder temperature in RCCI combustion led to a lower heat transfer through the cylinder wall, resulting in a higher BTE than the baseline CI combustion [41, 42]. However, at a very high premixed ratio ($r_p = 0.75$), a too slow fuel-air chemical kinetics resulted in an incomplete combustion. The differences between the BTE of RCCI combustion fueled with different fuel-pairs were not significant and followed a random variation pattern at different r_p. EGT was the next performance parameter, which is an indirect measure of the in-cylinder temperature. Figure 5 shows that the EGT of RCCI combustion at a lower premixed ratio ($r_p = 0.25$) was comparable to the baseline CI combustion. However, the EGT of RCCI combustion at a higher r_p was lower than the baseline CI combustion. With an increasing r_p of the LRF, the EGT of RCCI combustion reduced (especially for Methanol/diesel- and Ethanol/diesel-fueled RCCI combustion). Reduction in the EGT of Methanol/diesel- and Ethanol/diesel-fueled RCCI combustion was also attributed to the higher LHV of Methanol. However, EGT reduction was lower for Butanol/diesel-fueled RCCI combustion. This was in agreement with the combustion results where Butanol/diesel-fueled RCCI combustion exhibited similarity with the baseline CI combustion. Overall, performance characteristics showed that Methanol/diesel and Ethanol/diesel fuel-pairs at intermediate r_p were suitable for RCCI combustion.

3.3. Emissions Characterization

To compare the emission characteristics of baseline CI combustion and RCCI combustion using Methanol/diesel, Ethanol/diesel, and Butanol/diesel fuel-pairs at different r_p, concentrations of HC, CO, and NOx were measured using an exhaust gas emission analyzer. Raw data of these regulated emission species (in parts per million) were converted to their corresponding brake-specific mass emission (g/kWh) by using standard mathematical formulae [43].

Figure 6 shows that RCCI combustion led to significantly higher CO emission from Methanol/diesel, Ethanol/diesel, and Butanol/diesel fuel-pairs at different r_p than the baseline CI combustion mode. CO emission from the baseline CI combustion was significantly lower than the RCCI combustion at all r_p. Lower in-cylinder temperature and reduced global reactivity may be possible reasons for higher CO emission from the RCCI combustion. CO emission from RCCI combustion increased with increasing r_p of the LRF and reached more than 20 g/kWh at $r_p = 0.75$. Among different fuel-pairs, Methanol/diesel-fueled RCCI combustion emitted the lowest CO at lower r_p. However, Butanol/diesel-fueled RCCI combustion emitted the lowest CO at higher r_p. At lower r_p, the presence of Methanol improved the combustion characteristics due to fuel-bound oxygen; however, at higher r_p, a larger amount of Methanol resulted in a significantly lower in-cylinder temperature, which hampered the CO-to-CO_2 oxidation. Ethanol/diesel-fueled RCCI combustion emitted the highest CO at all r_p than the two other fuel-pairs. The relatively lower in-cylinder temperature due to moisture in Ethanol may be a possible reason, which is also visible in the EGT results (Figure 5). HC emissions were the other major pollutants emitted by the CI engines. Incomplete combustion of fuel due to lower in-cylinder temperatures, fuel trapped in the crevices, and flame quenching are the main reasons for HC emissions from the CI engines [39]. Figure 6 shows that HC emissions followed a similar trend as that of CO emission. RCCI combustion emitted significantly higher HC emissions than the baseline CI combustion, which increased with the increasing r_p of the LRF. Reduced global reactivity of fuel-air mixture and trapping of the LRF in the crevices during compression stroke were the main reasons for higher HC emissions at higher r_p. Among different fuel-pairs, Butanol/diesel-fueled RCCI combustion emitted lower HC than the two other fuel-pairs. Higher in-cylinder pressure (Figure 2) and temperature (Figure 5) of Butanol/diesel-fueled RCCI combustion (due to higher global reactivity than Methanol/diesel and Ethanol/diesel fuel-pairs) were the two factors responsible for this trend. Lower NOx emissions are an important feature of RCCI combustion. In CI engines, NOx formation is mainly affected by three factors, namely, higher in-cylinder temperature, the presence of oxygen, and time available for the reactions. Results show that RCCI combustion emitted lower NOx than the baseline CI combustion, which further reduced with an increasing r_p of the LRF (except for Butanol/diesel-fueled RCCI combustion at $r_p = 0.75$). The relatively lower in-cylinder temperature was the main reason for NOx reduction from the RCCI combustion. Among different fuel-pairs, Ethanol/diesel-fueled RCCI combustion emitted the lowest NOx; however, Butanol/diesel-fueled RCCI combustion emitted the highest NOx. The relatively higher global reactivity may be a possible reason for higher NOx emissions from Butanol/diesel-fueled RCCI combustion, which might be responsible for the relatively higher peak in-cylinder temperature than the two other fuel-pairs. Butanol/diesel-fueled RCCI combustion emitted a slightly higher NOx at $r_p = 0.75$, which may be due to the combined effect of higher in-cylinder temperature and the presence of oxygen in the test fuel. Overall, the emission characteristics showed that Methanol/diesel and Ethanol/diesel fuel-pairs at intermediate r_p are suitable for RCCI combustion.

3.4. Particulate Characterization

The detailed particulate analysis is an important aspect of this study. This section includes number-size distribution of particulates; number concentration of particles of different sizes such as nanoparticles ($D_p < 10$ nm), nucleation mode

FIGURE 6 CO, HC, and NOx emitted from the baseline CI combustion (red background) and RCCI combustion (green background) at different r_p of Methanol, Ethanol, and Butanol blended with mineral diesel at constant engine speed (1500 rpm) and low load (3 bar BMEP).

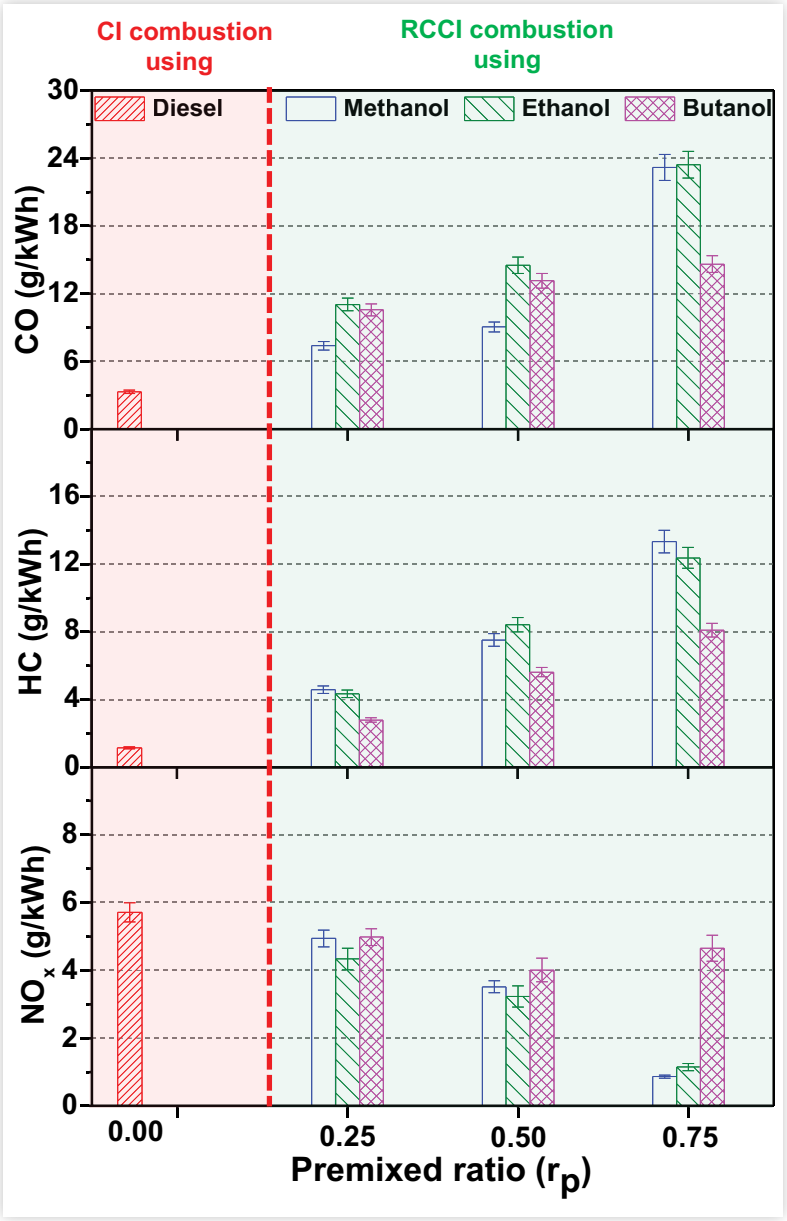

particles (NMP, 10 nm < D_p < 50 nm), and accumulation mode particles (AMP, 50 nm < D_p); total particle numbers (TPN); TPM; and count mean diameter (CMD) of particles. Correlation between TPM and NOx emissions showed a few important aspects of RCCI combustion fueled with different alcohol/diesel fuel-pairs.

Figure 7 shows the number-size distribution of particulates emitted from the baseline CI combustion and RCCI combustion fueled with Methanol, Ethanol, and Butanol at different r_p. Results showed that RCCI combustion fueled with different alcohol/diesel fuel-pairs emitted lower particulates than the baseline CI combustion. Similar findings related to LTC were reported in previous studies as well [44, 45, 46, 47, 48, 49, 50, 51]. There were many factors responsible for reducing particulates from RCCI combustion mode, among which improved charge homogeneity, higher fuel oxygen content, and higher fuel-air chemical kinetics were the important ones [44, 47, 50]. With an increasing r_p of the LRF, the particulate number-size distribution showed some interesting trends. At lower premixed ratios (r_p = 0.25 and 0.50), most particles emitted from RCCI combustion were in the AMP size range. At lower r_p, the dominant effect of oxygenated LRF was the main reason for the particulate reduction, which improved the particulate oxidation, and

FIGURE 7 Number-size distribution of particles emitted by the baseline CI combustion, and RCCI combustion at different r_p of Methanol, Ethanol, and Butanol blended with mineral diesel at constant engine speed (1500 rpm), and low load (3 bar BMEP).

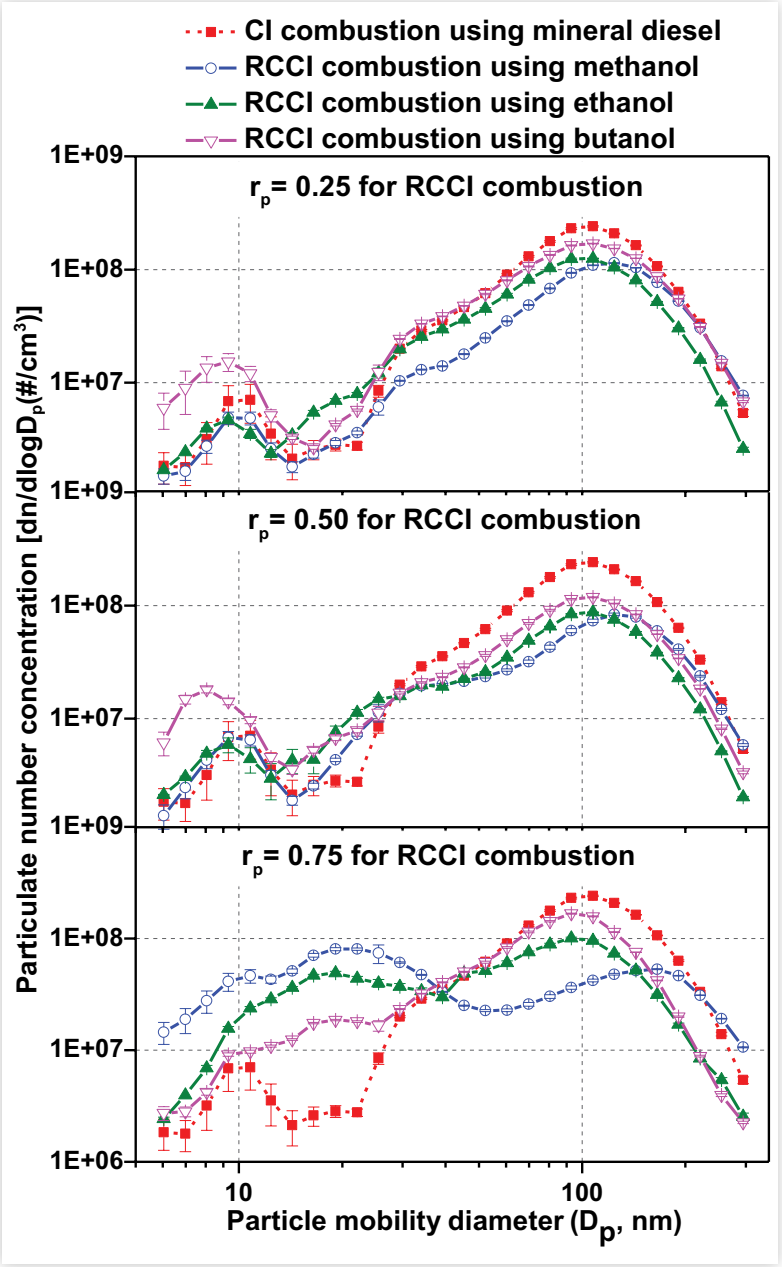

the relatively lower global reactivity provided more time for agglomeration. Storey et al. [45] also reported similar trends for oxygenated fuels in the RCCI combustion mode. At a higher premixed ratio (r_p = 0.75), the concentration of smaller particles increased significantly. The number-size distribution followed a pattern similar to SI engines, in which NMPs were higher than AMPs. There are many factors responsible for this trend. The relatively lower in-cylinder temperature might be a factor that could have prevented volatile species formation, resulting in a lower particle agglomeration tendency. Due to a lower in-cylinder temperature, significantly higher HC emissions contributed as nucleation sites for particle formation, which were emitted as NMPs in the exhaust. Northrop et al. [47] and Lucachick et al. [48] also reported similar attributes of LTC in particulate formation and growth. Homogeneous fuel-air mixing of the LRF might be another factor, which increased particulate nucleation and reduced accumulation.

RCCI combustion-fueled with different fuel-pairs showed variations in particulate characteristics at different r_p. At lower premixed ratios (r_p = 0.25 and 0.50), Methanol/diesel- and Ethanol/diesel-fueled RCCI combustion emitted lesser particulates than the baseline CI combustion in all size ranges. The presence of oxygen and lower carbon-to-hydrogen

ratio of the test fuel was the main reason for reducing particulate emission, which further decreased with increasing fuel oxygen content in the test fuels. At lower premixed ratios (r_p = 0.25 and 0.50), a slightly lower number concentration of particulates from Methanol/diesel-fueled RCCI combustion than the other fuel-pairs was another important observation. At lower r_p, a trade-off between the global reactivity (fuel-air chemical kinetics) and fuel properties was a main reason for such a trend. Due to increased fraction of the LRF, the presence of more oxygen in the combustion chamber resulted in quicker agglomeration and oxidation (up to a certain extent), resulting in more AMPs than the smaller particulates [51]. At lower r_p, Butanol/diesel-fueled RCCI combustion emitted a higher number of smaller particles than the other fuel-pairs. The combined effect of higher flame speed and improved combustion of Butanol/diesel fuel pair might be a possible reason for this trend, which promoted the pyrolysis of the lubricating oil, resulting in relatively higher NPs. These trends significantly changed at higher r_p, where the RCCI combustion emitted significantly higher NMPs than the baseline CI combustion. However, the number concentration of AMPs emitted from the RCCI combustion remained lower than the baseline CI combustion. At all r_p, particulate characteristics of Butanol/diesel-fueled RCCI combustion showed similarity with the baseline CI combustion; however, particulate characteristics of Methanol/diesel-fueled RCCI combustion were quite similar to the SI combustion [52]. At higher r_p, retarded combustion of Methanol/diesel- and Ethanol/diesel-fueled RCCI combustion was unable to complete the particulate growth due to the presence of relatively lower in-cylinder temperature; however, the presence of higher in-cylinder temperature in the Butanol/diesel-fueled RCCI combustion resulted in more agglomeration, leading to a higher concentration of AMPs.

Figure 8 shows variations in number concentrations of NPs, NMPs, and AMPs emitted from the baseline CI combustion and RCCI combustion fueled with Methanol/diesel, Ethanol/diesel, and Butanol/diesel fuel-pairs at different r_p. Results show that RCCI combustion emitted slightly higher NPs (especially at higher r_p) than the baseline CI combustion. With an increasing r_p of the LRF, NP emissions increased. Among different fuel-pairs, Butanol/diesel-fueled RCCI combustion emitted higher NPs than the Methanol/diesel- and Ethanol/diesel-fueled RCCI combustion (at r_p = 0.25 and 0.50); however, at r_p = 0.75, Methanol/diesel-fueled RCCI combustion emitted the highest number of NPs. The number concentration of NPs emitted from the RCCI combustion varied from ~ 5×10^7 to 1.5×10^8 particles per cm^3 of the raw exhaust.

The number concentration of NMPs also followed a similar trend as that of NPs. The number concentration of NMPs emitted from the RCCI combustion (at r_p = 0.25 and 0.50) was comparable to the number concentration of NMPs emanating from the baseline CI combustion (~2×10^8 particles per cm^3 of exhaust gas). However, NMPs from RCCI combustion increased significantly (~5×10^8 particles per cm^3 of exhaust gas) at a higher premixed ratio (r_p = 0.75). Among different fuel-pairs, Butanol/diesel-fueled RCCI combustion emitted the highest NMPs at r_p = 0.25 and 0.50; however, Methanol/diesel-fueled RCCI combustion emitted the highest NMPs at r_p = 0.75. The number concentration of AMPs was dominant in both baseline CI and RCCI combustion fueled with Methanol/diesel, Ethanol/diesel, and Butanol/diesel (except Methanol/diesel-fueled RCCI combustion at r_p = 0.75). Results show that the baseline CI combustion emitted more AMPs (~1.5×10^9 particles per cm^3 of exhaust gas) than the RCCI combustion (~1×10^9 particles per cm^3 of exhaust gas). With an increasing r_p of LRF, the number concentration of AMPs showed a different pattern for each fuel-pair. With an increasing r_p of LRF, Methanol/diesel-fueled RCCI combustion resulted in lower APMs. However, the number concentration of AMPs first decreased (up to r_p = 0.50) and then increased for Ethanol/diesel- and Butanol/diesel-fueled RCCI combustion. A relatively higher number concentration of AMPs from Butanol/diesel-fueled RCCI combustion than the other alcohols was an important observation, which was in agreement with the previous results reflecting that the Butanol/diesel-fueled RCCI combustion was similar to the baseline CI combustion.

Figure 9 shows variations in TPN, TPM, and CMD of particles emitted by the baseline CI combustion and the RCCI combustion fueled with Methanol/diesel, Ethanol/diesel, and Butanol/diesel-fueled fuel-pairs in different r_p. Results show that RCCI combustion emitted lower TPN than the baseline CI combustion. The presence of a homogeneous fuel-air mixture of the LRF and fuel-bound oxygen were the two important reasons for this behavior. With an increasing r_p of the LRF, the TPN first decreased (up to r_p = 0.50) and then increased at higher r_p. Dominant contribution of the premixed fuel-air mixture was the main reason for the reduced TPN of up to r_p = 0.50; however, at the higher r_p, a significant reduction in the in-cylinder temperature led to a higher degree of soot nucleation, which resulted in a higher TPN [49]. Among different alcohols, Butanol/diesel-fueled RCCI combustion emitted higher TPN than the TPN emitted by the Methanol/diesel- and Ethanol/diesel-fueled RCCI combustion.

TPM is another important parameter calculated by the number-size distribution of particulates by assuming that all particles emitted from the engine were spherical. The density of particulates was assumed to be constant [53]. Results show that the TPM emitted by the baseline CI combustion was higher than that by the RCCI combustion. The contribution of oxygenated LRF was the main reason for this trend, which promoted particulate oxidation. For all test fuels, TPM emitted by the RCCI combustion decreased with increasing r_p of the LRF. The absence of fuel-rich zones due to the dominant contribution of homogeneous LRF-air mixture may be a possible reason for TPM reduction at higher r_p. At r_p = 0.75, a difference trend of the TPN and TPM was an important observation. With an increasing r_p from 0.50 to 0.75, a TPN increased; however, the TPM was reduced. This was mainly due to formation of higher number of relatively smaller particles, which increased the TPN; however, their contribution to the TPM was not significant. The CMD of particles

FIGURE 8 Number concentrations of nanoparticles, nucleation mode particles, and accumulation mode particles emitted by the baseline CI combustion (red background) and RCCI combustion (green background) at different r_p of Methanol, Ethanol, and Butanol blended with mineral diesel at constant engine speed (1500 rpm), and low load (3 bar BMEP).

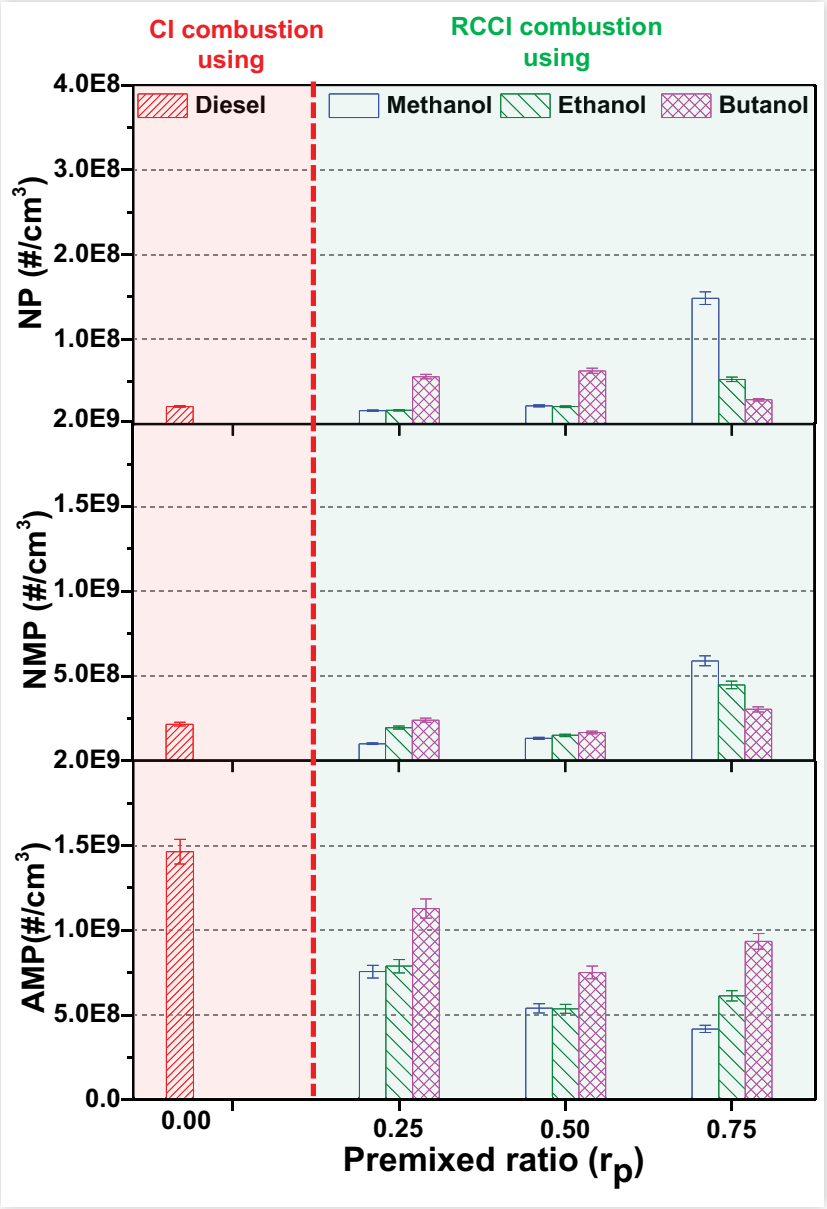

represents the average size of particulates emitted by the engine [54]. Results show that the CMD of particles emitted by RCCI combustion (especially up to r_p = 0.50) was comparable to the CMD of particles emitted by the baseline CI combustion. However, at r_p = 0.75, the CMD of particles emitted by the RCCI combustion was significantly lower (especially for Methanol/diesel- and Ethanol/diesel-fueled fuel-pair RCCI combustion) than the baseline CI combustion. With an increasing r_p, the CMD of particles emitted by RCCI combustion reduced. This trend was common for all fuel-pairs. However, it was more prominent for Methanol/diesel- and Ethanol/diesel-fueled RCCI combustion at the higher r_p. Methanol/diesel-fueled RCCI combustion at lower r_p resulted in a lower CMD of particles; however, at the higher r_p, Butanol/diesel-fueled RCCI combustion produced particles with higher CMD.

Figure 10 shows the qualitative correlation between the number and mass-size distribution of particles emitted by the CI and RCCI combustion modes. In this figure, PM mass-size distribution is shown on the Y-axis, and the PM number-size distribution is shown on the X-axis [55]. A lobe was plotted by joining the PM number and mass corresponding to each mean PM size in an increasing order ranging from 5.6 to 560 nm. The size and shape of the lobe reflect the relationship

FIGURE 9 TPN, TPM, and CMD of particles emitted by the baseline CI combustion (red background), and RCCI combustion (green background) at different r_p of Methanol, Ethanol, and Butanol blended with mineral diesel at constant engine speed (1500 rpm), and low load (3 bar BMEP).

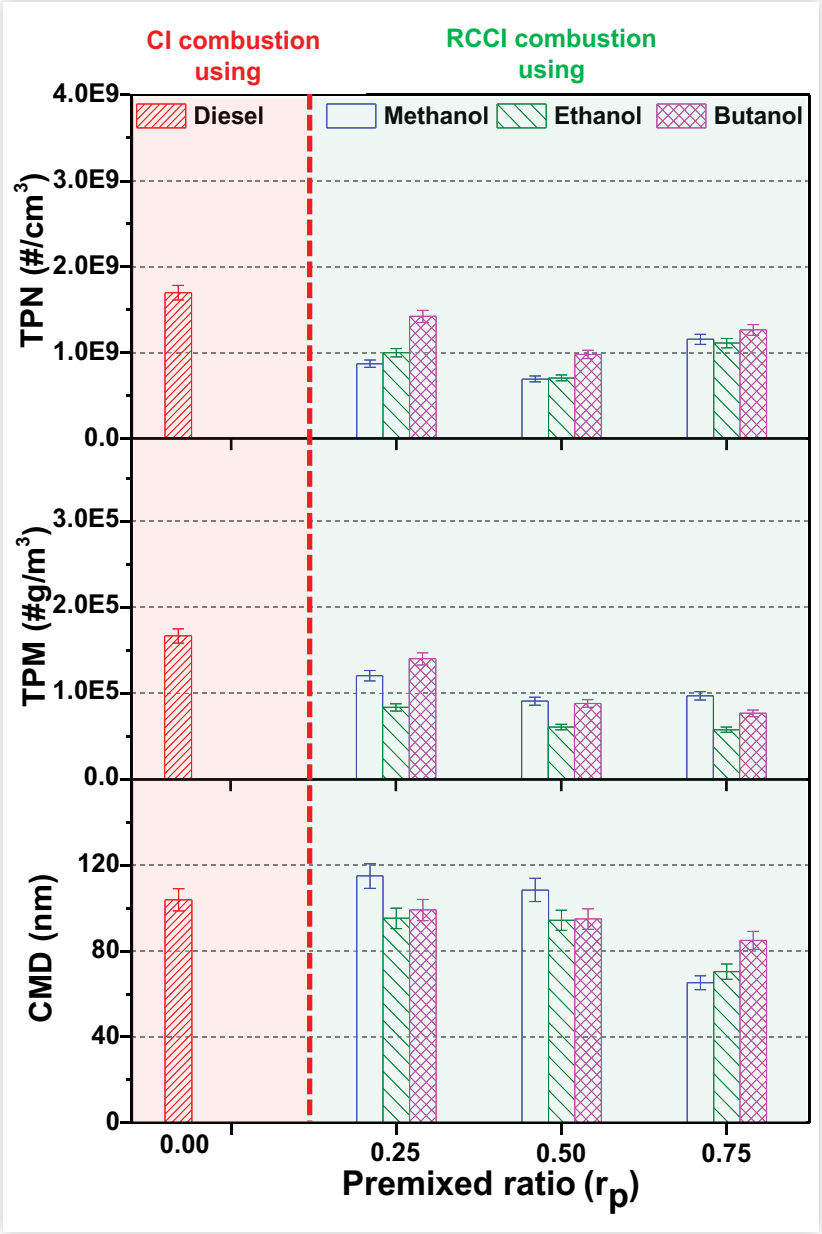

between the PM mass and PM numbers. A larger lobe indicates higher PM emissions in both numbers as well as mass. If the lobe is inclined toward the X-axis, this indicates the PM number's dominance; and the lobe's inclination toward the Y-axis indicates the dominance of PM mass.

Figure 10 shows different characteristics of particles emitted from RCCI combustion w.r.t. baseline CI combustion. Similar to previous results, this qualitative correlation also shows a relatively lower particulate emission from the RCCI combustion than the CI combustion, which was dominant at higher r_p. At higher r_p, a higher inclination of the correlation curves of Butanol/diesel and Ethanol/diesel fuel-pairs towards the X-axis shows the domination of particle number than the particle mass. However, the Methanol/diesel fuel-pair's correlation curve was more inclined toward the Y-axis, which reflects a domination of particle mass due to a relatively higher concentration of bigger particles (Figure 7). With increasing r_p, the mass of bigger particles emitted from Methanol/diesel-fueled RCCI combustion became more dominant; however the mass of smaller particles did not contribute significantly to the TPM. The similarity of the Butanol/diesel fuel-pair with CI combustion was also visible in these correlation plots.

FIGURE 10 Number-size and mass-size correlation of particles emitted by the baseline CI combustion, and RCCI combustion at different r_p of Methanol, Ethanol, and Butanol blended with mineral diesel at constant engine speed (1500 rpm), and low load (3 bar BMEP).

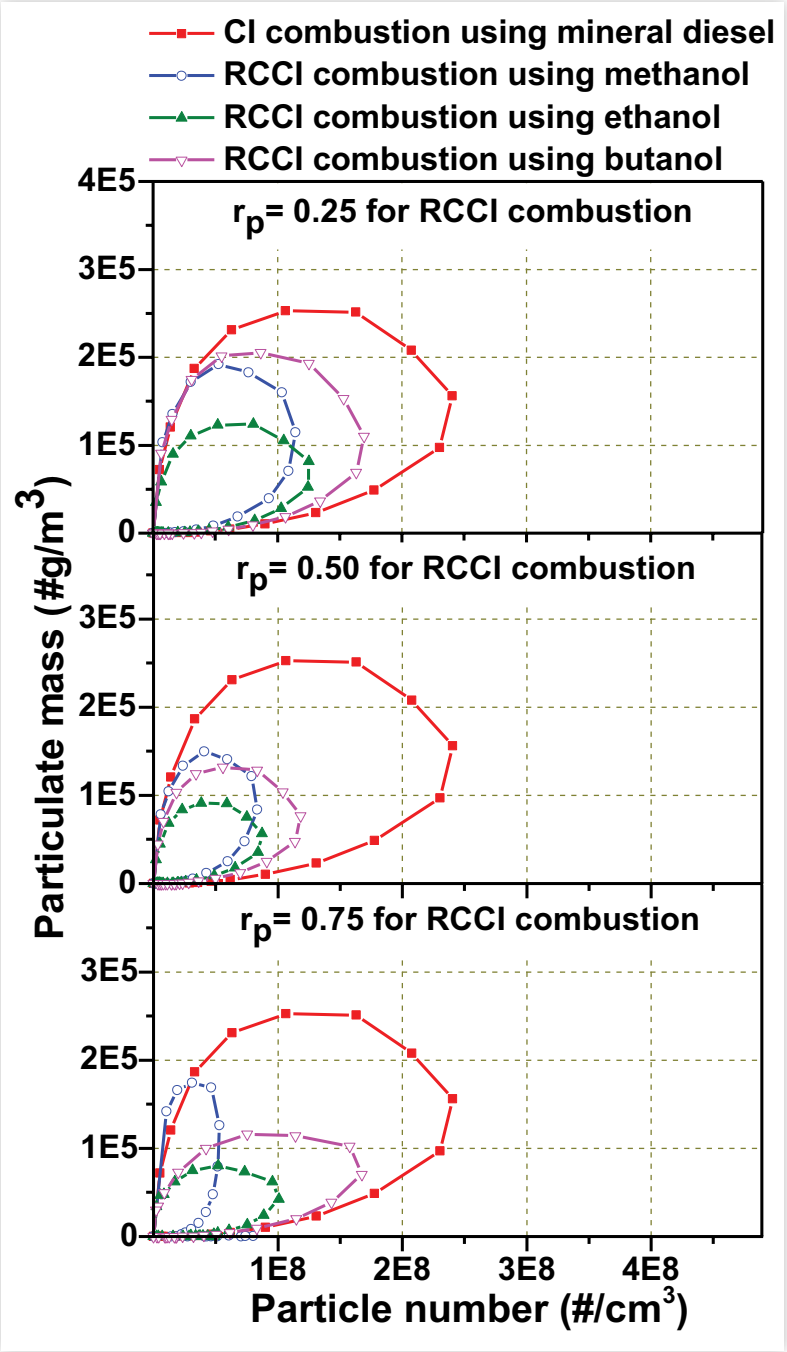

Figure 11 shows a correlation between the TPM (Y-axis) and the NOx (X-axis) emitted by the baseline CI combustion and the RCCI combustion fueled with Methanol/diesel, Ethanol/diesel, and Butanol/diesel fuel-pairs at different r_p. In this analysis, a rectangle with more height represents higher PM, and a wider rectangle represents higher NOx emissions. A smaller rectangle represents simultaneous reduction of NOx and PM emissions, which is desirable for the IC engines.

Figure 11 shows a simultaneous reduction of both TPM and NOx emissions in the RCCI combustion. At all r_p, TPM-NOx rectangles were inside the TPM-NOx rectangle of the baseline CI combustion. With increasing r_p, RCCI combustion showed dominant NOx reduction (especially for Methanol/diesel- and Ethanol/diesel-fueled RCCI combustion); however, TPM reduction was less significant. Among different alcohols, Methanol/diesel and Ethanol/diesel fuel-pairs were found to

FIGURE 11 Correlation between the TPM and NOx emissions by the baseline CI combustion, and RCCI combustion at different r_p of Methanol, Ethanol, and Butanol blended with mineral diesel at constant engine speed (1500 rpm), and low load (3 bar BMEP).

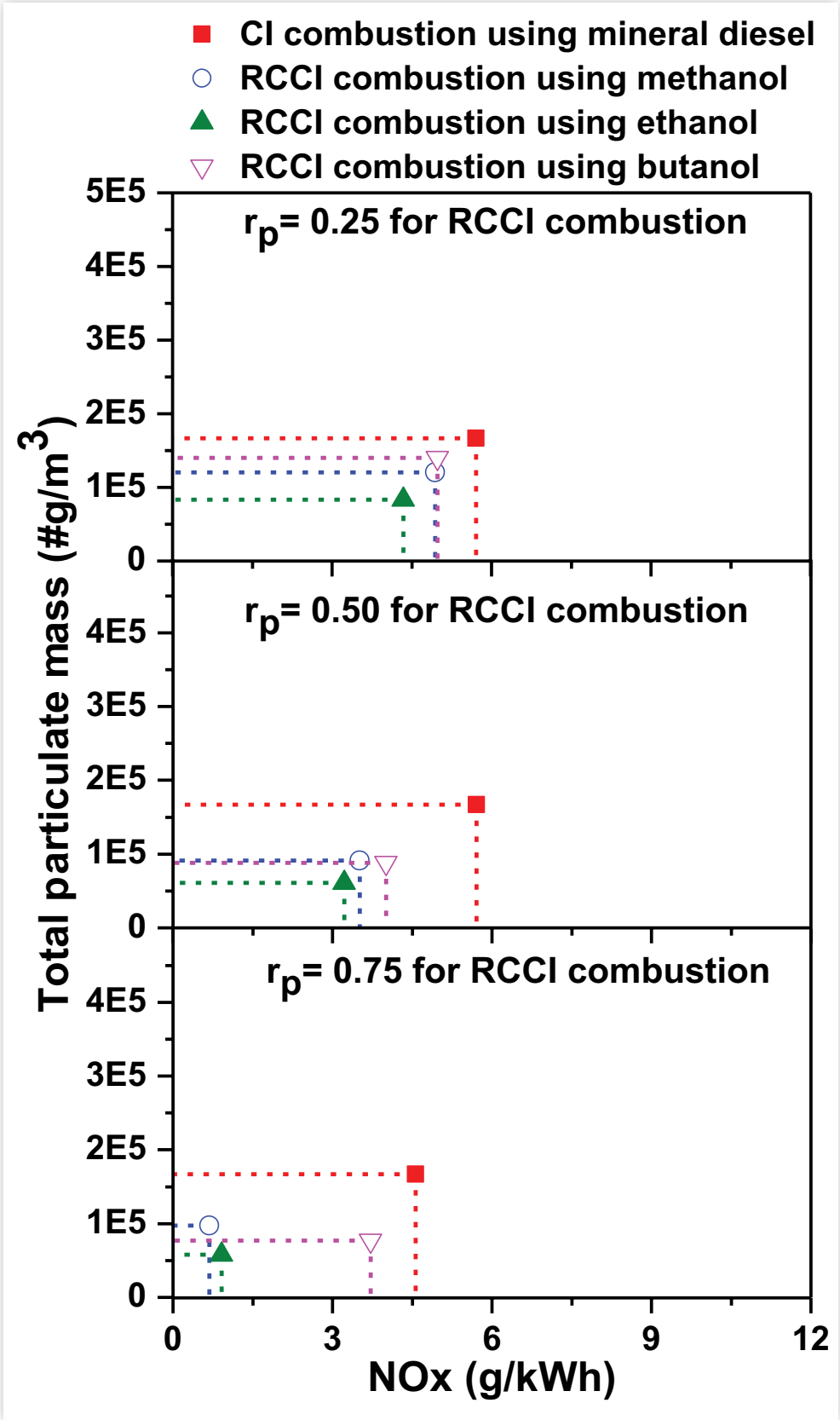

be more suitable for RCCI combustion because of the more stable combustion (Figure 2) and emission characteristics (Figure 4) than the Butanol/diesel fuel-pair.

4. Conclusions

This experimental study compared the feasibility and suitability of different primary alcohols, namely, Methanol, Ethanol, and Butanol as LRF and mineral diesel as HRF in RCCI combustion mode. RCCI combustion investigations were carried out at different r_p of LRF (r_p = 0.25, 0.50, and 0.75), and results were compared with the baseline CI combustion (r_p = 0.0). The effect of a relatively lower reactivity of primary alcohols was evident. However, the effect of moisture traces present in ethanol resulted in a significantly different RCCI mode combustion than the other alcohols. RCCI combustion exhibited a significantly retarded SoC and CP than the baseline CI combustion. The effect of a relatively lower fuel reactivity was dominant for Methanol and Ethanol; hence, they were more suitable LRFs for the RCCI combustion mode. Butanol exhibited a greater similarity with the baseline CI combustion due to its relatively higher reactivity than the other alcohols. The EGT of RCCI combustion fueled with different fuel-pairs was lower than the baseline CI combustion, which was also reflected in the NOx emission trends. Ethanol-diesel-fueled RCCI combustion exhibited relatively lower NOx emissions due to moisture traces in Ethanol, leading to a relatively lower peak in-cylinder temperature. NOx emissions from Butanol-diesel-fueled RCCI combustion were the highest among all primary alcohols tested. Particulates emitted by RCCI combustion mode were lower than the baseline CI combustion, and they further reduced with an increasing r_p of LRF. The dominant contribution of relatively smaller particles at higher r_p was an important finding of this study, which resulted in a lower reduction in TPN at higher r_p. However, their contribution to the TPM was less significant. TPM-NOx correlation showed the capability of simultaneous NOx-PM reduction in the RCCI combustion. Methanol and Ethanol were more suitable as LRF in the RCCI combustion mode than Butanol. The suitability of Ethanol and Butanol can be further improved by removing the moisture traces and by varying the fuel injection timing. Therefore, it can be concluded that these three primary alcohols can be utilized as LRF in RCCI combustion mode to resolve the issues of fossil fuel availability and emission control simultaneously. This study provided fundamental results that would be utilized in simulation studies for model validation and further research in the future.

Contact Information

Corresponding Author
akag@iitk.ac.in

References

1. Johnson, T., "Review of Diesel Emissions and Control," *SAE Int. J. Fuels Lubr.* 3, no. 1 (2010): 16-29, https://doi.org/10.4271/2010-01-0301.
2. Agarwal, A.K., Srivastava, D.K., Dhar, A., Maurya, R.K. et al., "Effect of Fuel Injection Timing and Pressure on Combustion, Emissions and Performance Characteristics of a Single Cylinder Diesel Engine," *Fuel* 111 (2013): 374-383.
3. Paykani, A., Kakaee, A., Rahnama, P., and Reitz, R.D., "Progress and Recent Trends in Reactivity-Controlled Compression Ignition Engines," *International Journal of Engine Research* 17, no. 5 (2016): 481-524.
4. Agarwal, A.K., Singh, A.P., and Maurya, R.K., "Evolution, Challenges and Path forward for Low Temperature Combustion Engines," *Progress in Energy and Combustion Sciences* 61 (2017): 1-56.
5. Singh, A.P. and Agarwal, A.K., "Partially Homogenous Charge Compression Ignition Engine Development for Low Volatility Fuels," *Energy and Fuels* 31, no. 3 (2017): 3164-3181.
6. Jain, A., Singh, A.P., and Agarwal, A.K., "Effect of Fuel Injection Parameters on Combustion Stability and Emissions of a Mineral Diesel Fueled Partially Premixed Charge Compression Ignition (PCCI) Engine," *Applied Energy* 190 (2017): 658-669.
7. Jain, A., Singh, A.P., and Agarwal, A.K., "Effect of Split Fuel Injection and EGR on NOx and PM Emission Reduction in a Low Temperature Combustion (LTC) Mode Diesel Engine," *Energy* 122 (2017): 249-264.
8. Dempsey, A., Walker, N., Gingrich, E., and Reitz, R.D., "Comparison of Low Temperature Combustion Strategies for Advanced Compression Ignition Engines with a Focus on Controllability," *Combust Sci Technol* 86, no. 2 (2014): 210e41.
9. Manente, V., Tunestal, P., and Johansson, B., "Partially Premixed Combustion at High Load Using Gasoline and Ethanol, a Comparison with Diesel," SAE Technical Paper 2009-01-0944, 2009, https://doi.org/10.4271/2009-01-0944.
10. Kokjohn, S.L. and Reitz, R.D., "Reactivity Controlled Compression Ignition and Conventional Diesel Combustion: A Comparison of Methods to Meet Light-Duty NOx and Fuel Economy Targets," *Int J Engine Res* 14, no. 5 (2013): 452-468.
11. Li, Y., Jia, M., Chang, Y., Liu, Y. et al., "Parametric Study and Optimization of a RCCI (Reactivity Controlled Compression Ignition) Engine Fueled with Methanol and Diesel," *Energy* 65, no. 11 (2014): 319-332.
12. Kokjohn, S., Reitz, R.D., Splitter, D., and Musculus, M., "Investigation of Fuel Reactivity Stratification for Controlling PCI Heat-Release Rates Using High-Speed Chemiluminescence Imaging and Fuel Tracer Fluorescence," *SAE Int. J. Eng.* 5, no. 2 (2012): 248-269, https://doi.org/10.4271/2012-01-0375.
13. Kokjohn, S., Hanson, R., Splitter, D., and Reitz, R., "Experiments and Modeling of Dual-Fuel HCCI and PCCI Combustion Using In-Cylinder Fuel Blending," SAE Technical Paper 2009-01-2647, 2009, https://doi.org/10.4271/2009-01-2647.
14. Kokjohn, S., Hanson, R., Splitter, D., Kaddatz, J. et al., "Fuel Reactivity Controlled Compression Ignition (RCCI) Combustion in Light- and Heavy-Duty Engines," SAE Technical Paper 2011-01-0357, 2011, https://doi.org/10.4271/2011-01-0357.

15. Dempsey, A.B., Walker, N.R., and Reitz, R., "Effect of Cetane Improvers on Gasoline, Ethanol, and Methanol Reactivity and the Implications for RCCI Combustion," *SAE Int. J. Fuels Lubr.* 6, no. 1 (2013): 170-187, https://doi.org/10.4271/2013-01-1678.
16. Reitz, R.D. and Ganesh Duraisamy, G., "Review of High Efficiency and Clean Reactivity Controlled Compression Ignition (RCCI) Combustion in Internal Combustion Engines," *Progress in Energy and Combustion Science* 46 (2015): 12-71.
17. Liu, H., Ma, G., Hu, B., Zheng, Z. et al., "Effects of Port Injection of Hydrous Ethanol on Combustion and Emission Characteristics in Dual-Fuel Reactivity Controlled Compression Ignition (RCCI) Mode," *Energy* 145 (2018): 592-602.
18. Martinez-Frias, J., Aceves, S.M., and Flowers, D.L., "Improving Ethanol Life Cycle Energy Efficiency by Direct Utilization of Wet Ethanol in HCCI Engines," *J. Energy Resour. Technol.* 129 (2007): 332.
19. Hanson, R., Kokjohn, S., Splitter, D., and Reitz, R., "An Experimental Investigation of Fuel Reactivity Controlled PCCI Combustion in a Heavy-Duty Engine," *SAE Int. J. Engines* 3, no. 1 (2010): 700-716, https://doi.org/10.4271/2010-01-0864.
20. Splitter, D.A., Hanson, R.M., Kokjohn, S.L., and Reitz, R.D., "Reactivity Controlled Compression Ignition (RCCI) Heavy-Duty Engine Operation at Mid-and High-Loads with Conventional and Alternative Fuels," SAE Technical Paper 2011-01-0363, 2011, https://doi.org/10.4271/2011-01-0363.
21. Curran, S., Hanson, R., and Wagner, R., "Effect of E85 on RCCI Performance and Emissions on a Multi-Cylinder Light-Duty Diesel Engine," SAE Technical Paper 2012-01-0376, 2012, https://doi.org/10.4271/2012-01-0376.
22. Dempsey, A.B., Adhikary, A.D., Viswanathan, S., and Reitz, R.D., "Reactivity Controlled Compression Ignition (RCCI) Using Premixed Hydrated Ethanol and Direct Injection Diesel," *ICEF* 60235 (2011): 963-975.
23. Zou, X., Wang, H., Zheng, Z., Reitz, R. et al., "Numerical Study of the RCCI Combustion Processes Fueled with Methanol, Ethanol, n-Butanol and Diesel," SAE Technical Paper 2016-01-0777, 2016, https://doi.org/10.4271/2016-01-0777.
24. Turner, M., "Review and Benchmarking of Alternative Fuels in Conventional and Advanced Engine Concepts with Emphasis on Efficiency, CO2, and Regulated Emissions," SAE Technical Paper 2016-01-0882, 2016, https://doi.org/10.4271/2016-01-0882.
25. Isik, M.Z. and Aydin, H., "Analysis of Ethanol RCCI Application with Safflower Biodiesel Blends in a High Load Diesel Power Generator," *Fuel* 184 (2016): 248-260.
26. Hanson, R.M., Kokjohn, S.L., Splitter, D.A., and Reitz, R.D., "An Experimental Investigation of Fuel Reactivity Controlled PCCI Combustion in a Heavy-Duty Engine," SAE Technical Paper 2010-01-0864, 2010, https://doi.org/10.4271/2010-01-0864.
27. Fang, W., Kittelson, D.B., and Northrop, W.F., "Optimization of Reactivity-Controlled Compression Ignition Combustion Fueled with Diesel and Hydrous Ethanol Using Response Surface Methodology," *Fuel* 160 (2015): 446-457.
28. Park, S.H., Yoon, S.H., and Lee, C.S., "Bioethanol and Gasoline Premixing Effect on Combustion and Emission Characteristics in Biodiesel Dual-Fuel Combustion Engine," *Applied Energy* 135 (2014): 286-298.
29. Hanson, R., Curran, S., Wagner, R., and Reitz, R., "Effects of Biofuel Blends on RCCI Combustion in a Light-Duty, Multi-Cylinder Diesel Engine," *SAE Int. J. Engines* 6, no. 1 (2013): 488-503, https://doi.org/10.4271/2013-01-1653.
30. Zheng, Z., Xia, M., Liu, H., Wang, X. et al., "Experimental Study on Combustion and Emissions of Dual Fuel RCCI Mode Fueled with Biodiesel/n-Butanol, Biodiesel/2,5-Dimethylfuran and Biodiesel/Ethanol," *Energy* 148 (2018): 824-838.
31. Prikhodko, V.Y., Curran, S.J., Barone, T.L., Lewis, S.A. et al., "Diesel Oxidation Catalyst Control of Hydrocarbon Aerosols from Reactivity Controlled Compression Ignition Combustion," in *ASME 2011 International Mechanical Engineering Congress and Exposition, IMECE*, Denver, CO, 2011, 2011-64147, 273-278.
32. Singh, A.P. and Agarwal, A.K., "Effect of Intake Charge Temperature and EGR on Biodiesel Fueled HCCI Engine," SAE Technical Paper 2016-28-0257, 2016, https://doi.org/10.4271/2016-28-0257.
33. Singh, A.P., Jain, A., and Agarwal, A.K., "Fuel-Injection Strategy for PCCI Engine Fueled by Mineral Diesel and Biodiesel Blends," *Energy and Fuels* 31, no. 8 (2017): 8594-8607.
34. Singh, A.P., Pal, P., Gupta, N.K., and Agarwal, A.K., "Particulate Emissions from Laser Ignited and Spark Ignited Hydrogen Fueled Engines," *International Journal of Hydrogen Energy* 42, no. 24 (2017): 15956-15965.
35. Yanowitz, J., Ratcliff, M.A., McCormick, R.L., Taylor, J.D. et al., "Compendium of Experimental Cetane Numbers," Technical Report, National Renewable Energy Laboratory, 2014.
36. Design Institute for Physical Property Data, *Data Compilation Tables of Properties of Pure Compounds* (New York: American Institute of Chemical Engineers, 1984)
37. "The Basis of This Table and Associated References Was Taken From: American Petroleum Institute (API), Alcohols and Ethers," Publication No. 4261, 2nd ed., Washington, DC, July 1988, Table B-1.
38. Singh, A.P. and Agarwal, A.K., "Diesoline, Diesohol, and Diesosene Fueled HCCI Engine Development," *Journal of Energy Resources Technology* 138 (2016): 052212-052211.
39. Heywood, J.B., *Internal Combustion Engine Fundamentals* (New York: McGraw-Hill Book Company, 1988)
40. Rassweiler, G. and Withrow, L., "Motion Pictures of Engine Flames Correlated with Pressure Cars," SAE Technical Paper 380139, 1938, https://doi.org/10.4271/380139.
41. Benajes, J., García, A., Monsalve-Serrano, J., and Sari, R.L., "Fuel Consumption and Engine-Out Emissions Estimations of a Light Duty Engine Running in Dual-Mode RCCI/CDC

with Different Fuels and Driving Cycles," *Energy* 157 (2018): 19-30.

42. Pan, S., Li, X., Han, W., and Huang, Y., "An Experimental Investigation on Multi-Cylinder RCCI Engine Fueled with 2-Butanol/Diesel," *Energy Conversion and Management* 154 (2017): 92-101.
43. Indian Standard IS: 14273, "Automotive Vehicles—Exhaust Emissions—Gaseous Pollutants from Vehicles Fitted with Compression Ignition Engines—Method of Measurement," Bureau of Indian Standards, New Delhi, India, 1999.
44. Thomas, J.J., Sabu, V.R., Nagarajan, G., Kumar, S. et al., "Influence of Waste Vegetable Oil Biodiesel and Hexanol on a Reactivity Controlled Compression Ignition Engine Combustion and Emissions," *Energy* 206 (2020): 118199.
45. Storey, J.M., Curran, S.J., Lewis, S.A., Barone, T.L. et al., "Evolution and Current Understanding of Physicochemical Characterization of Particulate Matter from Reactivity Controlled Compression Ignition Combustion on a Multicylinder Light-Duty Engine," *International Journal of Engine Research* 18, no. 5-6 (2017): 505-519.
46. Barone, T.L., Storey, J.M.E., Youngquist, A.D., and Szybist, J.P., "An Analysis of Direct-Injection Spark-Ignition (DISI) Soot Morphology," *Atmos Environ* 49 (2012): 268-274.
47. Northrop, W.F., Madathil, P.V., Bohac, S.V., and Assanis, D.N., "Condensational Growth of Particulate Matter from Partially Premixed Low Temperature Combustion of Biodiesel in a Compression Ignition Engine," *Aerosol Sci Tech* 45, no. 1 (2011): 26-36.
48. Lucachick, G., Curran, S., Storey, J., Prikhodko, V. et al., "Characterization of Semi-Volatile Nanoparticles from Single and Dual-Fuel Low Temperature Combustion in Compression Ignition Engines," *Aero Sci Tech* 50 (2016): 436-447.
49. Dempsey, A., Curran, S., Storey, J., Eibl, M. et al., "Particulate Matter Characterization of Reactivity Controlled Compression Ignition (RCCI) on a Light Duty Engine," SAE Technical Paper 2014-01-1596, 2014, https://doi.org/10.4271/2014-01-1596.
50. Yang, B., Li, S., Zheng, Z., and Yao, M., "A Comparative Study on Different Dual-Fuel Combustion Modes Fuelled with Gasoline and Diesel," SAE Technical Paper 2012-01-0694, 2012, https://doi.org/10.4271/2012-01-0694.
51. Seong, H., Lee, K., Choi, S., Adams, C. et al., "Characterization of Particulate Morphology, Nanostructures, and Sizes in Low-Temperature Combustion with Biofuels," SAE Technical Paper 2012-01-0441, 2012, https://doi.org/10.4271/2012-01-0441.
52. Singh, A.P., Pal, P., and Agarwal, A.K., "Comparative Particulate Characteristics of Hydrogen, CNG, HCNG, Gasoline and Diesel-Fueled Engines," *Fuel* 185, no. 1 (2016): 491-499.
53. "Engine Exhaust Particle Sizer™ Spectrometer Model 3090," Operation and Service Manual, TSI, March 2009.
54. Agarwal, A.K., Ateeq, B., Gupta, T., Singh, A.P. et al., "Toxicity and Mutagenicity of Exhaust from Compressed Natural Gas: Could This Be a Clean Solution for Megacities with Mixed-Traffic Conditions?" *Environmental Pollution* 239 (2018): 499-511.
55. Shukla, P.C., Gupta, T., Gupta, N., and Agarwal, A.K., "A Qualitative Correlation between Engine Exhaust Particulate Number and Mass Emissions," *Fuel* 202 (2017): 241-245.